An Experimental Study on the Shear Behavior of T-Beams Strengthened with Fiber Reinforced Polymers

Jauhari Prasetiawan
Civil Engineering Department, Faculty of Engineering, Al-Azhar Islamic University, Indonesia | Civil Doctoral Program in Civil Engineering, Faculty of Engineering, Sultan Agung Islamic University, Indonesia
jauhariprasetiawan@unizar.ac.id (corresponding author)

Antonius
Doctoral Program in Civil Engineering, Faculty of Engineering, Sultan Agung Islamic University, Indonesia
antonius@unissula.ac.id

Prabowo Setiyawan
Doctoral Program in Civil Engineering, Faculty of Engineering, Sultan Agung Islamic University, Indonesia
prabowo@unissula.ac.id

Auliya Isti Makrifa
Civil Engineering Department, Faculty of Engineering, Al-Azhar Islamic University, Indonesia
auliya@unizar.ac.id

Received: 3 December 2025 | Revised: 17 December 2025 and 2 January 2026 | Accepted: 9 January 2026

 DOI: https://doi.org/10.48084/etasr.16582

ABSTRACT

This study presents an experimental and analytical investigation of shear strengthening for Reinforced Concrete (RC) T-beams using externally bonded carbon-fiber-reinforced polymer in U-wrap and side-bonded configurations and externally anchored steel strips. Fourteen identical T-beams were tested under four-point bending to create a shear-critical region near the support. The variables were the strengthening system, the number of carbon-fiber layers (one to three), and the presence or absence of internal stirrups (6 mm diameter at 200 mm spacing). Concrete compressive strength was 25 MPa. The carbon-fiber material had an ultimate tensile strength of 4900 MPa, an elastic modulus of 240 GPa, and a nominal thickness of 0.167 mm per layer. Load and deflection were recorded with a load cell and displacement transducers to evaluate stiffness and ductility, while crack development and failure modes were documented. All strengthened beams increased the maximum load relative to the reference beam with stirrups. U-wrap strengthening with stirrups provided the highest gain (40%–44%). Side-bonded strengthening showed lower gains due to premature end-debonding. Anchored steel strips achieved comparable enhancement (up to 43%) and promoted a shear–flexure response. PΨ Cross Section Analysis predictions were compared with experimental shear capacities to identify conservatism or overestimation and support calibration for design.

Keywords-RC T-beams; shear strengthening; FRP; U-wrap; side-bonded; anchored steel strips; reinforced concrete cross section analysis

I. INTRODUCTION

RC is widely used in buildings and bridges. However, shear failure in beams, particularly T beams, is brittle and may occur suddenly [1]. The presence of a flange complicates the flow of shear stresses, and as a result unstrengthened T beams can exhibit a reduction in shear capacity of approximately 20%-5% compared to rectangular beams with the same reinforcement ratio. This behavior highlights the need for appropriate and effective strengthening strategies [2] such as externally bonded

reinforcement. Conventional strengthening methods are often expensive, time-consuming, and disruptive. Thus, FRPs constitute a solution due to their high strength and installation ease, typically applied as U-wrap or side-bonded systems [3]. U-wraps can increase shear capacity by about 40%–85%, whereas side-bonded FRP often provides only 25%–45% because of end debonding and limited effective strain [4, 5]. As a result, experimental shear strength (V_u) is frequently lower than code-based predictions (ϕV_n), especially for T-beams [6, 7]. In parallel, externally anchored steel strips offer a more ductile alternative and can enhance shear capacity by about 30–60%. Nevertheless, studies on T-beams remain limited despite the strong influence of flange geometry [8]. Research highlights limited FRP–steel comparisons in T-beams and potential overestimation for multi-layer FRP in current codes [9]. Therefore, this study provides new experimental data on T-beams strengthened with FRP and external steel strips, evaluating the reliability of current design provisions for such members.

II. LITERATURE REVIEW

Shear strengthening research has emphasized external systems such as FRP and steel strips. Most studies have focused on rectangular beams, offering limited understanding of the shear behavior of T beams, particularly regarding the influence of internal stirrups and the agreement between theoretical predictions and experimental shear capacities. In general, FRP U-wrap configurations are considered highly effective, whereas side-bonded FRP systems tend to be less efficient because their contribution is often limited by premature end debonding and peeling mechanisms [10, 11]. More advanced approaches, including near-surface-mounted and embedded through-section FRP systems, have been developed to enhance bond performance and delay debonding; however, these techniques are more invasive and, thus, less practical for retrofitting existing structures [12]. For T sections, full-scale experimental evidence remains limited, while the complex shear stress field significantly affects the performance of externally bonded FRP, particularly at the flange to web transition and in relation to debonding behavior. Moreover, most studies examine only a single FRP strengthening system and rarely provide direct and consistent comparisons between U wrap and side-bonded configurations applied to geometrically identical T beams. Externally anchored steel strips are also seldom included as an alternative strengthening option. Although steel plates or strips can substantially increase shear capacity when debonding is controlled through mechanical anchorage or welded connectors, their effectiveness as external stirrups in T beams, both with and without internal stirrups, has not been systematically investigated [13]. To address these research gaps, the present study investigates shear-critical RC T beams subjected to a two-point loading configuration. A single, comprehensive experimental program is used to directly compare the following strengthening systems:

- FRP U wrap configurations, tested with and without internal stirrups.
- Side-bonded FRP systems using 1-3 layers, tested with and without internal stirrups.
- Externally anchored steel strips, tested with and without internal stirrups [14, 15].

The structural performance of the strengthened beams is evaluated by measuring shear capacity and overall load-carrying behavior, assessing ductility based on load deflection responses, and identifying crack development and failure modes through visual observations [16, 17]. In addition, the performance of current design models is assessed by comparing theoretical shear capacities (ϕV_n), calculated in accordance with relevant design provisions [6, 7], with the experimentally obtained shear capacities (V_u). This comparison is used to identify trends of conservatism or overestimation and to support the calibration of practical design approaches for the shear strengthening of RC T beams [20, 21]. The theoretical shear capacities were calculated using the Reinforced Concrete Cross Section Analysis (RCCSA) program based on section geometry, material properties, stirrup configuration, and FRP/steel-strip layout, as well as nominal and design shear strengths. The experimental results were then compared with RCCSA predictions using the response characteristics to evaluate model accuracy, identify deviation trends for each type of strengthening, and develop practical recommendations for the shear strengthening of RC T-beams.

A. Materials and Equipment

The current study used RC T-beams made with 25 MPa concrete and conventional steel reinforcement, including Ø6 mm stirrups at 200 mm spacing for specimens with internal shear reinforcement. External strengthening employed Estop/Estowrap FRP, the ultimate tensile strength of FRP (f_{uf}) = 4900 MPa, the elastic modulus of FRP (E_f) = 240000 MPa, FRP thickness (t_f) = 0.167 mm/layer, and structural steel grade SS37 steel strips (50 mm × 5 mm) anchored with SS41 anchors and resin, with epoxy/resin used as the bonding agent. Concrete cylinders were cast for quality-control tests, and loading was applied using a 50-ton hydraulic jack, as depicted in Figure 1.

Fig. 1. Hydraulic jack and loading frame.

The loading frame is a full-scale portal rig anchored to the laboratory floor through a 14 mm thick steel base plate [18]. The base plate is bolted to the concrete floor, and two vertical columns are connected by a WF steel beam forming the top cross-member. The applied load P was measured using a 50-ton load cell (or pressure gauge) installed directly above the hydraulic jack according to [19] and Figure 2.

Fig. 2. Load Cell and LVDT.

Linear Variable Differential Transformers (LVDTs) were installed at selected points along the span and near the supports to measure the vertical deflections of the beam specimens. A data logger was used to continuously record the load and deflection readings from the hydraulic jack, load cell, and LVDTs.

Additional equipment included a concrete mixer, beam and cylinder molds, compaction tools, curing tanks, and auxiliary tools such as a grinder, drill, wire brush, scale, oven, and others. All tested T beams had identical cross-sectional dimensions, consisting of web width $(b_w) = 150$ mm, overall depth $(h) = 300$ mm, flange thickness $(t_f) = 100$ mm, and total length $(L) = 1300$ mm. The longitudinal reinforcement layout, including both tension and compression bars, was kept the same for all specimens. Variations were introduced only in the shear reinforcement, by providing or omitting stirrups, and in the type and configuration of external strengthening, namely FRP U wrap, side-bonded FRP, and steel strips. For the U wrap configuration [20], FRP strips were applied to three sides of the beam section, with specified strip spacing and 1-3 FRP layers depending on the specimen designation. In the side-bonded configuration, FRP sheets were bonded only to the web faces of the beam, arranged in vertical or inclined patterns with defined spacing. Steel strips were installed along the beam web, with a width of 50 mm and a thickness of 5 mm, and were anchored to the concrete using SS41 steel anchors and resin.

B. Loading and Support Configuration

The beam was supported on two simple supports in a pinned and roller configuration. It included a left overhang of 0.1 m, a clear span of 0.8 m between supports A and B, and a right overhang of 0.4 m. Loading was applied through two concentrated loads. The load P_1 was applied at 0.4 m from the left support A, corresponding to 0.5 m from the left end of the beam, while the load P_2 was applied 0.35 m from the right support B, corresponding to 1.25 m from the left end. This loading arrangement created a shear critical region near support B, which was the primary focus of the shear strengthening investigation. Support reactions were determined using static equilibrium to calculate the shear forces at the critical section.

1) Preparation and Casting of Test Specimens

Reinforcement cages were fabricated according to the design drawings, including longitudinal bars and stirrups where applicable. The beam and cylinder molds were cleaned, oiled, and filled with 25 MPa concrete, which was vibrated for compaction. After about 24 h, the specimens were demolded and water-cured until testing (at least 28 days).

2) Installation of FRP and Steel Strip Strengthening

After the concrete reached the target age and strength, the strengthening zone was roughened by chiseling/grinding and cleaned to remove laitance and debris [21]. For FRP, a primer was applied, the sheets were cut to size, epoxy was spread, and FRP was bonded and rolled to remove air bubbles. For steel strips, anchor holes were drilled, strips were installed using resin and SS41 anchors according to the specified spacing and quantity, and all systems were left to cure fully in accordance with the manufacturer's recommendations.

3) Instrumentation and Testing

As shown in Figures 3 and 4 [22], the beam was mounted on the loading frame with two supports, A and B, spaced according to the test setup. A hydraulic jack and load cell were installed to apply the concentrated loads, P_1 and P_2. LVDTs or dial gauges were placed at selected points along the span and near the supports to measure vertical deflections. Loading was applied incrementally, and at each load step, the applied load, deflections at all measuring points, and the initiation and development of crack patterns were recorded. The test was continued until beam failure, indicated by a significant load drop or large deformation. The maximum recorded load was used to determine the experimental shear capacity (V_u).

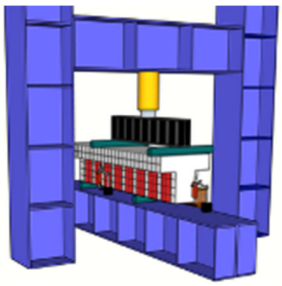

Fig. 3. Experimental test setup (a).

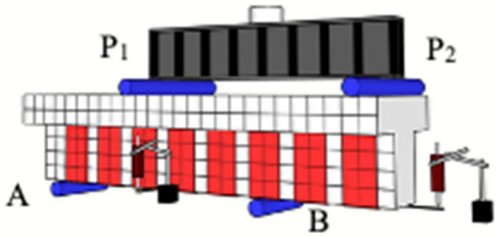

Fig. 4. Test setup (b).

C. Processing and Analysis of Experimental Data

The experimental shear capacity (V_u) was derived from the maximum test load (P_{max}) using static equilibrium based on the loading and support configuration (e.g., shear near support B from support reactions and overhang effects). Load–deflection curves were used to evaluate ductility and post-peak response. Crack patterns were then analyzed to classify the failure mode and assess the effect of strengthening, while all (V_u) values were compiled in a summary table.

D. Theoretical Analysis Using RCCSA

Each beam was modeled in RCCSA using the T-section geometry, concrete strength, longitudinal reinforcement, stirrup details, and the properties of FRP or steel strips treated as additional reinforcement according to the strengthening layout. For FRP, key inputs included (f_{uf}) and (E_f), strain limits (t_f), installation angle, number of layers, and strip width/spacing. RCCSA provided the nominal shear capacity (ϕV_n), and these values were tabulated alongside the experimental shear capacities (V_u).

E. Comparison and Deviation Evaluation

For each beam, the following ratio is calculated:

$$R = \frac{\phi V_n}{V_u} \quad (1)$$

The ratio (R) was evaluated for each strengthening group (FRP U-wrap with/without stirrups, side-bonded FRP with/without stirrups, steel strips, and control beams) to identify cases of good agreement ($R \approx 1$), conservative predictions ($R < 1$), and overestimation ($R \gg 1$), Deviations were interpreted in terms of effective FRP strain assumptions, debonding not captured by the model, diagonal cracking effects, material/detailing variability, and the limitations of sectional analysis. These findings were used to propose practical recommendations, including correction/reduction factors for RCCSA and the most effective strengthening configurations for RC T-beams in shear.

III. RESULTS AND DISCUSSION

All measurements were recorded during loading and verified for consistency to assess the influence of the strengthening variables on beam performance.

A. Material Data

The cylinder compression test shows an initially elastic, nearly linear stress–deflection response, followed by nonlinear behavior as microcracking develops and stiffness decreases. The concrete reaches a peak stress of about 25 MPa at a deflection of approximately 8 mm—9 mm, after which the curve exhibits a short plateau and then softens, indicating compressive failure and post-peak degradation. The steel tensile test exhibits a typical elastic–yield response. Stress increases linearly in the elastic range up to about 280 MPa, then the curve bends as yielding begins at roughly 8 mm–10 mm displacement, with stress rising more gradually toward an ultimate level of about 410 MPa.

B. Beam Test Results

Overall, as portrayed in Figures 5-8, the crack pattern in the strengthened beams indicates a shear failure influenced by flexure (shear–flexure behavior). Initial flexural cracks formed in the tensile zone and then propagated into diagonal cracks within the shear-critical region. With strengthening, the initiation and widening of diagonal cracks were better controlled, shifting the response from brittle shear toward a more stable shear–flexure mechanism in which flexural action contributes to crack development and final failure.

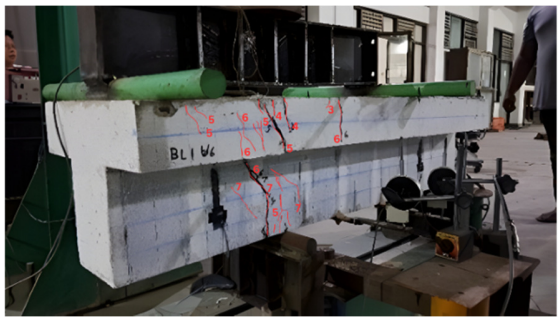

Fig. 5. Test documentation for specimen U-Wrap.

Fig. 6. Test documentation for specimen BL3-U6-f25.

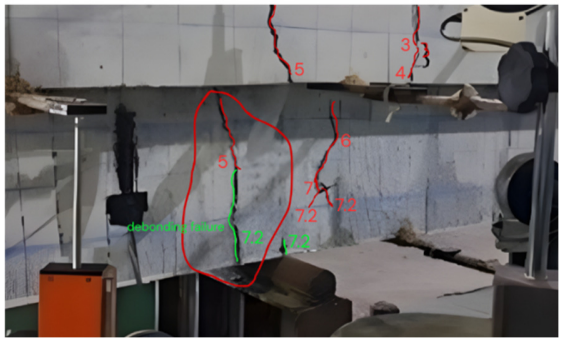

Fig. 7. Test documentation for specimen side-bonded.

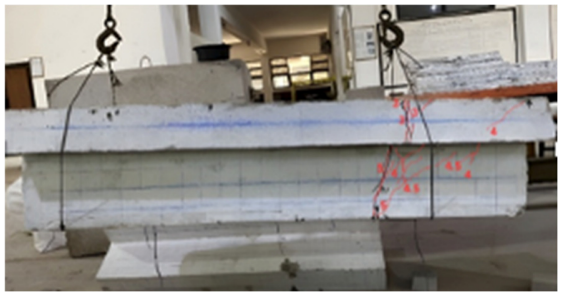

Fig. 8. Test documentation for specimen BLNS-0-f25.

C. Shear Capacity Enhancement Due to FRP

Each normal-strength concrete T beam specimen was identified using a three-part code separated by hyphens. The first part, "BL#", denotes the specimen number and the number of FRP layers applied. The second part indicates the strengthening configuration and the stirrup condition, where U represents an FRP U wrap, II denotes side-bonded FRP, and

the accompanying number specifies the stirrup diameter in mm. The final part indicates concrete compressive strength, $f25$, corresponding to a design compressive strength $f25 = f_c'25$ MPa. For example, specimen BL1-U6-f25 represents a normal-strength concrete T beam strengthened with one layer of FRP in a U wrap configuration, reinforced with Ø6 mm internal stirrups, and cast with concrete having $f_c' = 25$MPa. Specimen BLNS-0-f25 denotes a beam with conventional Ø6 mm stirrups at 200 mm spacing, but without any external strengthening, and serves as the stirrup-only control specimen. In contrast, BLNTS-0-f25 refers to a plain T beam without internal stirrups and without external strengthening, representing the most significant unstrengthened condition.

TABLE I. PERCENTAGE INCREASE IN MAXIMUM LOAD

No	Specimen code	Maximum load P_{max} (kN)	Maximum deflection Δ (mm)	Percentage effect of strengthening (%)
1	BL1-U6-f25	71.51	5.647	40.77%
2	BL2-U6-f25	73.21	16.380	44.11%
3	BL3-U6-f25	69.8	8.980	37.4%
4	BL1-II6-f25	63.35	14.760	24.7%
5	BL2-II6-f25	69.17	12.680	36.16%
6	BL3-II6-f25	72.18	12.480	42.09%
7	BL1-U0-f25	70.32	9.147	38.43%
8	BL2-U0-f25	62.54	8.293	23.11%
9	BL3-U0-f25	72.84	9.140	43.39%
10	BL1-II0-f25	65.09	9.424	28.13%
11	BL2-II0-f25	68.58	7.622	35%
12	BL3-II0-f25	60.9	7.622	19.88%
13	BLNS-0-f25	50.8	7.600	0%
14	BLNTS-0-f25	44.3	5.833	-12.8%

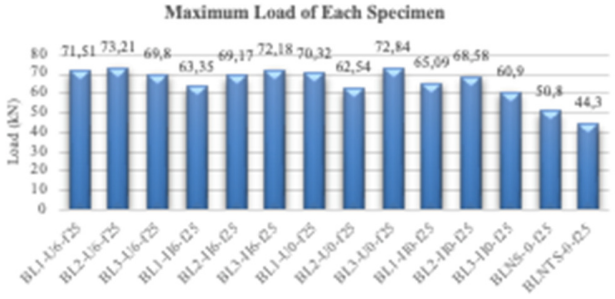

Fig. 9. Maximum load of each specimen.

Based on Table I and Figures 9-10, all strengthening configurations increased the maximum load compared to the unstrengthened reference specimens, confirming that shear capacity is dependent on the applied strengthening system. The FRP U-wrap combined with stirrups produced the largest improvement, about 40%–44%, and achieved the highest capacities among all groups, with the maximum load of 73.21 kN, demonstrating the effectiveness of three-sided confinement. Side-bonded FRP specimens with stirrups showed slightly lower but still relatively high capacities, indicating that U-wrap provides better confinement and bond performance than two-sided bonding. Steel-strip strengthening also provided a substantial increase; specimens with stirrups reached an improvement, and the best steel-strip configuration without FRP attained 72.84 kN, showing that anchored steel strips or related detailing can significantly enhance capacity. In contrast, the control beams (BLNS-0-f25 = 50.8 kN and BLNTS-0-f25 = 44.3 kN) exhibited the lowest capacities, highlighting the benefit of external strengthening when properly designed and installed.

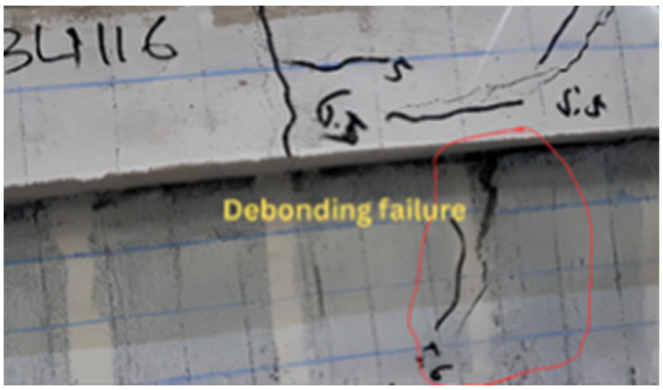

Fig. 10. Debonding failure.

For beams strengthened with side-bonded FRP and internal stirrups, the increase in shear capacity ranged from 24.7% to 42.09%, indicating that web side strengthening can be effective when properly detailed. In contrast, side-bonded FRP without internal stirrups resulted in lower capacity gains, ranging from 19.88%-35%, which highlights the important role of stirrups in mobilizing and enhancing the contribution of external FRP. The reference baseline specimen was the unstrengthened beam with Ø6 mm stirrups at 200 mm spacing (BLNS-0-f25), which exhibited a maximum load of 50.8 kN and was taken as the 0% reference. In comparison, the beam without stirrups and without external strengthening (BLNTS-0-f25) reached a maximum load of only 44.3 kN, corresponding to a 12.8% reduction in capacity, demonstrating the significant loss of shear resistance when internal shear reinforcement is absent. Figure 11 compares the load–deflection responses of all beam variants under two-point loading. Each curve reflects the initial stiffness (initial slope), peak capacity (maximum load), and post-peak response.

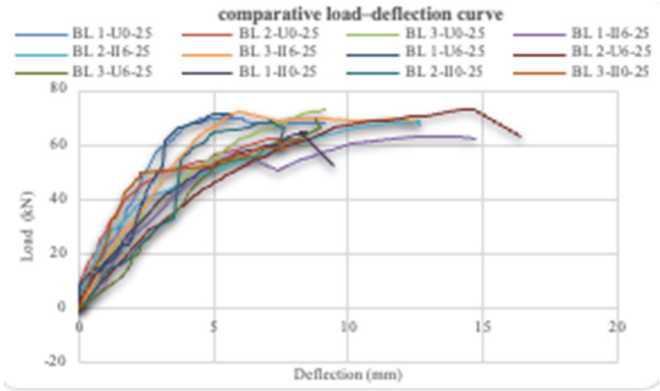

Fig. 11. Comparative load–deflection curves for all strengthened specimens.

TABLE II. ULTIMATE LOAD CAPACITY (PU) AND DUCTILITY OF THE T-BEAMS

Kode Benda U_{ji}	Pu (kN)	Py (kN)	Δu (mm)	Δy (mm)	μΔ = Δu/Δy
BL 1-II0-25	65.09	48.82	8.23	1.70	4.84
BL 2-II0-25	68.58	51.44	7.08	1.40	5.05
BL 3-II0-25	60.90	45.68	7.39	2.21	3.34
BL 1-U0-25	70.32	52.74	5.32	1.47	3.62
BL 2-U0-25	62.54	46.91	7.28	1.91	3.82
BL 3-U0-25	72.84	54.63	9.14	1.88	4.86
BL 1-II6-25	63.35	47.51	12.56	3.32	3.78
BL 2-II6-25	69.17	51.88	12.66	4.98	2.54
BL 3-II6-25	72.18	54.14	4.00	1.02	3.93
BL 1-U6-25	71.51	53.63	5.21	1.38	3.78
BL 2-U6-25	73.21	54.91	14.64	1.82	8.04
BL 3-U6-25	69.80	52.35	8.82	2.05	4.30
BLNTS-0-25	44.30	33.23	1.68	0.79	2.12
BLNS-0-25	50.80	38.10	5.08	1.73	2.94

The ductility results indicate that all external strengthening systems enhance both the ultimate load capacity (P_u) and ductility of the T-beams compared to the control specimens. The beam without stirrups and without external strengthening exhibits the lowest performance, with (P_u) =44.3 kN and a ductility index of only 2.12. Providing internal stirrups alone increases the ultimate load to 50.8 kN and improves the ductility to μΔ =2.94. For beams strengthened with side-bonded FRP and no internal stirrups, (P_u) increases to 60.9 kN–68.58 kN, while ductility improves to μΔ =3.34–5.05, with the maximum value of 5.05. When internal stirrups are added, the ultimate load further increases to 63.35–72.18 kN; however, ductility generally decreases to 2.54–3.93 due to the increased stiffness of the strengthened beams. FRP U-wrap strengthening provides a superior overall response. For beams without stirrups, (P_u) the ranges from 62.54 to 72.84 kN, with ductility values between 3.62 and 4.86. The combination of U-wrap FRP and internal stirrups yields the best performance, achieving ultimate loads exceeding 69 kN and the highest ductility, with μΔ =8.04 for the specimen strengthened with 2 layers of FRP. Therefore, the configuration using 2 layers of FRP U-wrap in conjunction with internal stirrups can be considered the most effective strengthening system, as it provides both the highest load capacity and the greatest post-yield deformation capability.

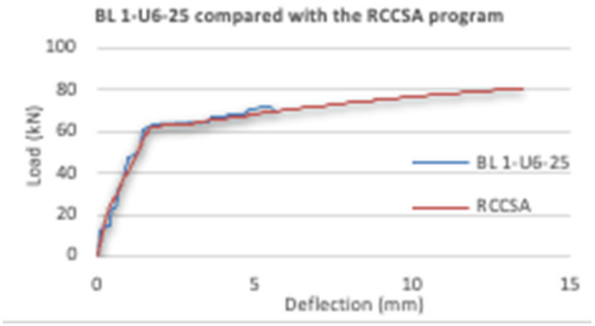

Fig. 12. Load–deflection curve of BL1-U6-25 compared with RCCSA program.

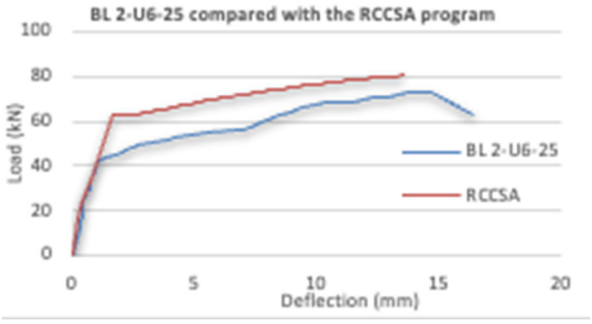

Fig. 13. Load–deflection curve of BL 2-U6-25 compared with RCCSA program.

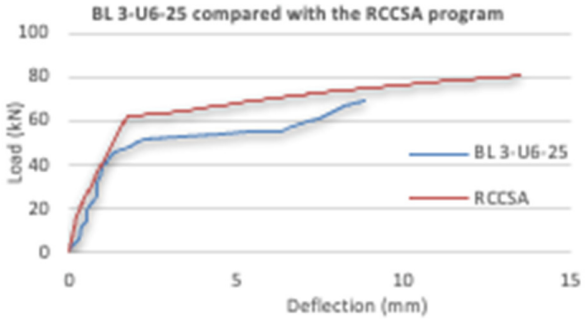

Fig. 14. Load–deflection curve of BL 3-U6-25 compared with RCCSA program.

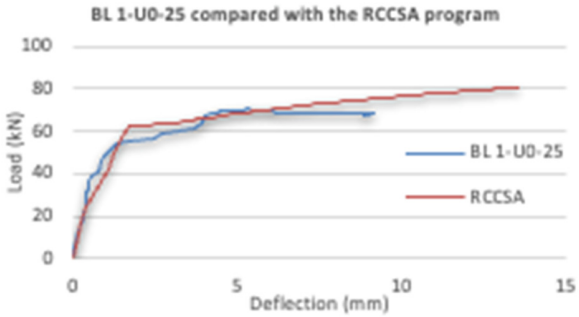

Fig. 15. Load–deflection curve of BL 1-U0-25 compared with RCCSA program.

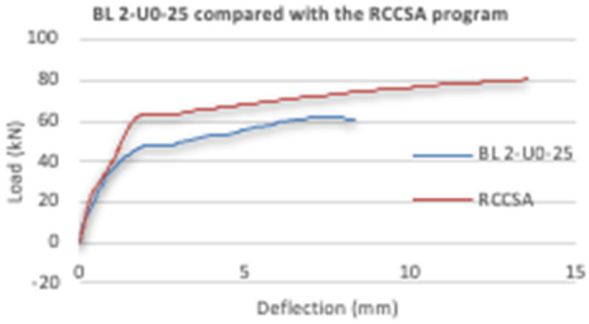

Fig. 16. Load–deflection curve of BL 2-U0-25 compared with RCCSA program.

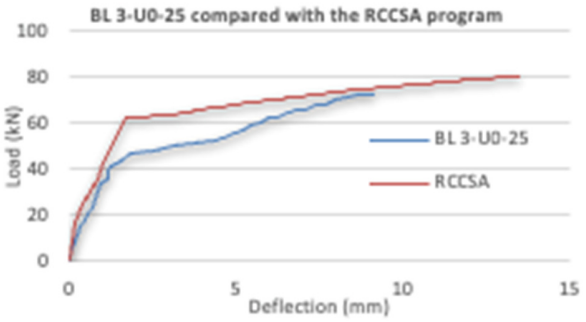

Fig. 17. Load–deflection curve of BL 3-U0-25 compared with RCCSA program.

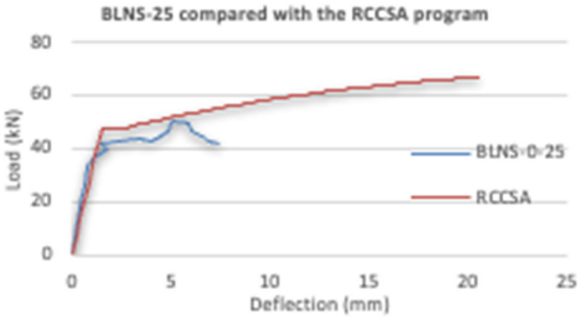

Fig. 18. Load–deflection curve of BLNS-25 compared with RCCSA program.

Across all specimens, as shown in Figures 12-18, the load–deflection responses indicate that RCCSA predicts the initial elastic behavior with reasonable accuracy. Up to approximately 60 kN–65 kN, the experimental and analytical curves are closely aligned, demonstrating that the program can adequately capture the gross flexural stiffness of the T-beams. Beyond this load level, the experimental curves exhibit stiffness degradation and gradual flattening, whereas the RCCSA predictions continue to increase more smoothly. As a result, the program systematically overestimates post-cracking stiffness and ultimate load capacity, primarily because it does not account for diagonal cracking, FRP debonding, or bond-slip effects. Beams strengthened with FRP U-wraps and internal stirrups (BL1-U6-25, BL2-U6-25, and BL3-U6-25) achieved the highest load capacities and the largest deflections, with specimen BL2-U6-25 showing the most pronounced ductile response. This behavior confirms the effectiveness of full U-wrap strengthening combined with internal stirrups in enhancing ductility. In contrast, beams strengthened with U-wrap FRP without stirrups (BL1-U0-25 and BL2-U0-25), as well as the control beam (BLNS-0-25), exhibited earlier stiffness degradation and lower ultimate capacities. These results highlight the significant benefits of external strengthening, while also indicating that further calibration of RCCSA is required for accurate prediction of the behavior of FRP-strengthened RC T-beams.

IV. CONCLUSION

Overall, the experimental results confirm that external strengthening significantly improves the shear performance of Reinforced Concrete (RC) T-beams, with the/their magnitude depending on the strengthening configuration and the presence of internal stirrups. Compared to the stirrup-controlled reference beam, the strengthened specimens achieved increases in maximum load ranging from 19.88% to 44.11%, with the highest gain obtained by the FRP U-wrap specimen (44.11%), followed by the anchored steel-strip specimen (43.39%) and the side-bonded specimen (42.09%). FRP U-wrap provided the most reliable and highest peak enhancement because it effectively confined the web and better controlled diagonal cracking. Side-bonded FRP showed the most variable performance and was particularly sensitive to end-debonding, reaching the lowest improvement in 19.88%. Increasing the number of FRP layers improved shear capacity in a nonlinear manner, with diminishing returns at higher layers, likely due to interlayer slip. Anchored steel strips consistently increased capacity from 37.4% up to 43.39%, and tended to fail in a shear–flexure mode, indicating that the anchorage system helped mitigate debonding. For beams without stirrups, strengthening remained effective relative to the no-stirrup control, producing increases of approximately 37.47%–64.42%. However, the cracking response and failure tendency were more brittle than in beams with stirrups. In general, external strengthening shifted the failure mechanism from brittle shear toward shear–flexure, with U-wrap and steel strips providing better crack control, while side-bonded FRP was predominantly governed by debonding.

ACKNOWLEDGMENT

The authors would like to express their gratitude to Al-Azhar Islamic University (UNIZAR) and the Faculty of Engineering, UNIZAR, for their support of this research.

REFERENCES

[1] C. E. Chalioris, A. G. Zapris, and C. G. Karayannis, "U-Jacketing Applications of Fiber-Reinforced Polymers in Reinforced Concrete T-Beams against Shear—Tests and Design," *Fibers*, vol. 8, no. 2, Feb. 2020, Art. no. 13, https://doi.org/10.3390/fib8020013.

[2] C. E. Chalioris, P.-M. K. Kosmidou, and N. A. Papadopoulos, "Investigation of a New Strengthening Technique for RC Deep Beams Using Carbon FRP Ropes as Transverse Reinforcements," *Fibers*, vol. 6, no. 3, Sept. 2018, Art. no. 52, https://doi.org/10.3390/fib6030052.

[3] F. Bianchi, R. Nascimbene, and A. Pavese, "Experimental vs. Numerical Simulations: Seismic Response of a Half Scale Three-Storey Infilled RC Building Strengthened Using FRP Retrofit," *Open Civil EngineeringOpen Civil Engineering*, vol. 11, no. 1, Dec. 2017, https://doi.org/10.2174/1874149501711011158.

[4] Y. H. Mugahed Amran *et al.*, "RC beam strengthening using hinge and anchorage approach," *Results in Materials*, vol. 5, Mar. 2020, Art. no. 100047, https://doi.org/10.1016/j.rinma.2019.100047.

[5] C. Pellegrino and C. Modena, "FRP Shear Strengthening of RC Beams with Transverse Steel Reinforcement," *Journal of Composites for Construction*, May 2002, https://doi.org/10.1061/~ASCE!1090-0268~2002!6:2~1!.

[6] ACI 440.2R-17: Guide for the Design and Construction of Externally Bonded FRP Systems for Strengthening Concrete Structures. American Concrete Institute, 2017.

[7] SNI 2847-2019 Persyaratan Beton Struktural Untuk Bangunan Gedung. Indonesia: Standar Nasional Indonesia, 2019.

[8] M. A. Khan, "Towards progressive debonding in composite RC beams subjected to thermo-mechanical bending with boundary constraints – A new analytical solution," *Composite Structures*, vol. 274, Oct. 2021, Art. no. 114334, https://doi.org/10.1016/j.compstruct.2021.114334.

[9] A. G. Razaqpur, R. Cameron, and A. A. B. Mostafa, "Strengthening of RC beams with externally bonded and anchored thick CFRP laminate," *Composite Structures*, vol. 233, Feb. 2020, Art. no. 111574, https://doi.org/10.1016/j.compstruct.2019.111574.

[10] R. Al-Shamayleh, H. Al-Saoud, M. Abdel-Jaber, and M. Alqam, "Shear and flexural strengthening of reinforced concrete beams with variable compressive strength values using externally bonded carbon fiber plates," *Results in Engineering*, vol. 14, June 2022, Art. no. 100427, https://doi.org/10.1016/j.rineng.2022.100427.

[11] A. O. Ismael and A. R. Yousif, "Shear Strengthening of Reinforced Concrete Beams Using CFRP Strips," *Eurasian Journal of Science and Engineering*, vol. 9, no. 3, pp. 1–12, Dec. 2023, https://doi.org/10.23918/eajse.v9i3p01.

[12] A. S. Abdulrahman and M. R. A. Kadir, "Behavior and flexural strength of fire damaged high strength reinforced rectangular concrete beams after strengthening with CFRP laminates," *Ain Shams Engineering Journal*, vol. 13, no. 6, Nov. 2022, Art. no. 101767, https://doi.org/10.1016/j.asej.2022.101767.

[13] A. Bahrami, M. Ghalla, G. Elsamak, M. Badawi, E. A. Mlybari, and F. A. Abdelmgeed, "Various configurations of externally bonded strain-hardening cementitious composite reducing shear failure risk of defected RC beams," *Frontiers in Materials*, vol. 11, Oct. 2024, https://doi.org/10.3389/fmats.2024.1373292.

[14] A. Benzaamia, M. Ghrici, R. Rebouh, T. Sivenas, and P. G. Asteris, "Shear strength modeling for reinforced concrete beams strengthened with externally bonded fiber-reinforced polymer using machine learning," *Structures*, vol. 76, June 2025, Art. no. 108954, https://doi.org/10.1016/j.istruc.2025.108954.

[15] A. Abadel *et al.*, "Experimental study of shear behavior of CFRP strengthened ultra-high-performance fiber-reinforced concrete deep beams," *Case Studies in Construction Materials*, vol. 16, June 2022, Art. no. e01103, https://doi.org/10.1016/j.cscm.2022.e01103.

[16] X. Liu, O. Karaghool, G. E. Thermou, and J. Yu, "Experimental investigation on shear strengthening of RC beams using advanced fibre-reinforced cementitious composites," *Case Studies in Construction Materials*, vol. 23, Dec. 2025, Art. no. e05032, https://doi.org/10.1016/j.cscm.2025.e05032.

[17] S. Azhar, S. Sugiman, Z. Omar, and H. Ahmad, "Experimental investigations of strengthened beam with co-cured carbon FRP and mussel shell-modified epoxy," *Ain Shams Engineering Journal*, vol. 16, no. 10, Oct. 2025, Art. no. 103563, https://doi.org/10.1016/j.asej.2025.103563.

[18] Y. Ma *et al.*, "Research on the structural strength of medium and low speed maglev vehicle levitation frame based on full-scale test bench," *Engineering Failure Analysis*, vol. 180, Oct. 2025, Art. no. 109901, https://doi.org/10.1016/j.engfailanal.2025.109901.

[19] A. I. Naji and M. Al-Shamaa, "Structural behavior of innovative castellated steel beams: experimental and numerical analysis of double and zigzag castellated patterns," *Results in Engineering*, vol. 27, Sept. 2025, Art. no. 106259, https://doi.org/10.1016/j.rineng.2025.106259.

[20] F. A. Megahed, M. H. Seleem, A. A. M. Badawy, and I. A. Sharaky, "The flexural response of RC beams strengthened by EB/NSM techniques using FRP and metal materials: a state-of-the-art review," *Innovative Infrastructure Solutions*, vol. 8, no. 11, Oct. 2023, Art. no. 289, https://doi.org/10.1007/s41062-023-01245-z.

[21] H. Hasan and M. H. Al-Farttoosi, "Investigation of the Experimental Shear Resistance of RC T-beams after Strengthening with Carbon Fiber-Reinforced Polymer (CFRP) Bars," *Engineering, Technology & Applied Science Research*, vol. 14, no. 1, pp. 12608–12614, Feb. 2024, https://doi.org/10.48084/etasr.6578.

[22] J. Prasetiawan, A. Amir, and P. Setiyawan, "Experimental Study Of Simple Cyclic Testing On Reinforced Beam Using Fiber Reinforced Polymers (FRP)," *IOP Conference Series: Earth and Environmental Science*, vol. 1321, no. 1, Dec. 2024, Art. no. 012047, https://doi.org/10.1088/1755-1315/1321/1/012047.